The Astrophysical Journal, 672:1159–1166, 2008 January 10
© 2008. The American Astronomical Society. All rights reserved. Printed in U.S.A.

PARALLAX AND LUMINOSITY MEASUREMENTS OF AN L SUBDWARF

Adam J. Burgasser,[1] Frederick J. Vrba,[2] Sébastien Lépine,[3] Jeffrey A. Munn,[2] Christian B. Luginbuhl,[2] Arne A. Henden,[4] Harry H. Guetter,[2] and Blaise C. Canzian[5]

Received 2007 July 19; accepted 2007 September 10

ABSTRACT

We present the first parallax and luminosity measurements for an L subdwarf, the sdL7 2MASS J05325346+8246465. Observations conducted over 3 years by the USNO infrared astrometry program yield an astrometric distance of 26.7 ± 1.2 pc and a proper motion of 2.6241″ ± 0.0018″ yr^{-1}. Combined with broadband spectral and photometric measurements, we determine a luminosity of $\log L_{\rm bol}/L_\odot = -4.24 \pm 0.06$ and $T_{\rm eff} = 1730 \pm 90$ K (the latter assuming an age of 5–10 Gyr), comparable to mid-type L field dwarfs. Comparison of the luminosity of 2MASS J05325346+8246465 to theoretical evolutionary models indicates that its mass is just below the sustained hydrogen-burning limit, and is therefore a brown dwarf. Its kinematics indicate a ~110 Myr, retrograde Galactic orbit that is both eccentric (3 kpc $\lesssim R \lesssim$ 8.5 kpc) and extends well away from the plane ($\Delta Z = \pm 2$ kpc), consistent with membership in the inner halo population. The relatively bright *J*-band magnitude of 2MASS J05325346+8246465 implies significantly reduced opacity in the 1.2 μm region, consistent with inhibited condensate formation as previously proposed. Its as yet unknown subsolar metallicity remains the primary limitation in constraining its mass; determination of both parameters would provide a powerful test of interior and evolutionary models for low-mass stars and brown dwarfs.

Subject headings: stars: chemically peculiar — stars: fundamental parameters — stars: individual (2MASS J05325346+8246465) — stars: low-mass, brown dwarfs — subdwarfs

Online material: color figures

1. INTRODUCTION

The lowest luminosity stars and brown dwarfs are among the most useful probes of planetary, stellar, and Galactic processes. With hydrogen-burning lifetimes far in excess of a Hubble time (e.g., Laughlin et al. 1997) and space densities that exceed those of hotter stars, low-mass dwarfs are ubiquitous in the disk, thick-disk, and halo populations (e.g., Dahn et al. 1995; Reid et al. 2002; Digby et al. 2003; Cruz et al. 2007) and may host the bulk of terrestrial planets in the Galaxy (e.g., Boss 2006; Tarter et al. 2007). The steady cooling of brown dwarfs over time makes them useful chronometers for coeval clusters (Bildsten et al. 1997; Stauffer et al. 1998), and these sources probe star formation down to its lowest mass limit (Luhman et al. 2007 and references therein). Observations of cool brown dwarfs provide empirical constraints on atmospheric chemical models, opacities, and dynamics (e.g., Ackerman & Marley 2001; Lodders 2002; Helling et al. 2004) and facilitate studies of hot exoplanetary atmospheres (e.g., Baraffe et al. 2002).

Over the past decade, hundreds of low-mass stars and brown dwarfs have been identified by wide-field optical and near-infrared surveys such as the Two Micron All Sky Survey (2MASS; Skrutskie et al. 2006), the Sloan Digital Sky Survey (SDSS; York et al. 2000), and the Deep Near Infrared Survey of the Southern Sky (DENIS; Epchtein et al. 1997). These discoveries include members of two new spectral classes, the L dwarfs and T dwarfs (Kirkpatrick 2005 and references therein).[6] As the number of low-luminosity dwarfs grows, distinct populations of "peculiar" sources are being found that exhibit unusual surface gravities (e.g., Kirkpatrick et al. 2006), metallicities (e.g., Burgasser et al. 2003; Lépine et al. 2003), or atmospheric structures (e.g., Cruz et al. 2003, 2007; Knapp et al. 2004). One such population is the L subdwarf class (Burgasser et al. 2005), the metal-poor counterparts to solar metallicity field L dwarfs and the low-temperature extension of the M subdwarf sequence (Gizis 1997). L subdwarfs are distinguished from L dwarfs by the presence of relatively enhanced metal hydride absorption bands (CaH, FeH, CrH) and metal lines (Ca I, Ti I, Fe I) and reduced metal oxide absorption (TiO, VO; Mould 1976). They also exhibit exceptionally blue near-infrared colors ($J - K_s \lesssim 0$ compared to $J - K_s \approx 1.5$–2.5) caused by strong collision-induced H_2 absorption (Linsky 1969; Saumon et al. 1994; Borysow et al. 1997). Their halo or thick-disk kinematics (Burgasser et al. 2003; Reiners & Basri 2006) indicate an origin early in the Galaxy's history. L subdwarfs are useful for studying metallicity effects on cool atmospheric chemistry, particularly at temperatures in which photospheric condensates first become an important source of opacity (Ackerman & Marley 2001; Allard et al. 2001; Burrows et al. 2006). Like L dwarfs, they may also span the metal-dependent hydrogen-burning mass limit (Burgasser et al. 2003), and are therefore probes of low-mass star formation in the metal-poor halo. However, L subdwarfs are also exceptionally rare. Only four are currently known, identified serendipitously in the 2MASS (Burgasser et al. 2003; Burgasser 2004), SDSS (T. Sivarani et al. 2008, in preparation), and SUPERBLINK (Lépine et al. 2003) surveys.

Understanding the physical characteristics of metal-poor low-mass stars and brown dwarfs requires the characterization of basic

[1] Massachusetts Institute of Technology, Kavli Institute for Astrophysics and Space Research, Building 37, Room 664B, 77 Massachusetts Avenue, Cambridge, MA 02139; ajb@mit.edu.

[2] US Naval Observatory, Flagstaff Station, 10391 West Naval Observatory Road, Flagstaff, AZ 86001.

[3] Department of Astrophysics, Division of Physical Sciences, American Museum of Natural History, Central Park West at 79th Street, New York, NY 10024.

[4] American Association of Variable Star Observers (AAVSO), 25 Birch Street, Cambridge, MA 02138-1205.

[5] L-3 Communications/Brashear, 615 Epsilon Drive, Pittsburgh, PA 15238.

[6] A current list of known L and T dwarfs is maintained at http://dwarfarchives.org.

Report Documentation Page

Form Approved
OMB No. 0704-0188

Public reporting burden for the collection of information is estimated to average 1 hour per response, including the time for reviewing instructions, searching existing data sources, gathering and maintaining the data needed, and completing and reviewing the collection of information. Send comments regarding this burden estimate or any other aspect of this collection of information, including suggestions for reducing this burden, to Washington Headquarters Services, Directorate for Information Operations and Reports, 1215 Jefferson Davis Highway, Suite 1204, Arlington VA 22202-4302. Respondents should be aware that notwithstanding any other provision of law, no person shall be subject to a penalty for failing to comply with a collection of information if it does not display a currently valid OMB control number.

1. REPORT DATE	2. REPORT TYPE	3. DATES COVERED
10 JAN 2008		**00-00-2008 to 00-00-2008**

4. TITLE AND SUBTITLE	5a. CONTRACT NUMBER
Parallax And Luminosity Measurements Of An L Subdwarf	5b. GRANT NUMBER
	5c. PROGRAM ELEMENT NUMBER
6. AUTHOR(S)	5d. PROJECT NUMBER
	5e. TASK NUMBER
	5f. WORK UNIT NUMBER
7. PERFORMING ORGANIZATION NAME(S) AND ADDRESS(ES) **US Naval Observatory,Flagstaff Station 10391 West Naval Observatory Road,Flagstaff,AZ,86001**	8. PERFORMING ORGANIZATION REPORT NUMBER
9. SPONSORING/MONITORING AGENCY NAME(S) AND ADDRESS(ES)	10. SPONSOR/MONITOR'S ACRONYM(S)
	11. SPONSOR/MONITOR'S REPORT NUMBER(S)

12. DISTRIBUTION/AVAILABILITY STATEMENT
Approved for public release; distribution unlimited

13. SUPPLEMENTARY NOTES
The Astrophysical Journal, 672:1159-1166, 2008 January 10

14. ABSTRACT

15. SUBJECT TERMS

16. SECURITY CLASSIFICATION OF:			17. LIMITATION OF ABSTRACT	18. NUMBER OF PAGES	19a. NAME OF RESPONSIBLE PERSON
a. REPORT **unclassified**	b. ABSTRACT **unclassified**	c. THIS PAGE **unclassified**	**Same as Report (SAR)**	**9**	

TABLE 1
USNO Astrometric and Photometric Measurements for 2MASS J0532+8246

Parameter	Value
π_{rel}	36.3 ± 1.6 mas
π_{abs}	37.5 ± 1.7 mas
μ	2.6241″ ± 0.0018″ yr^{-1}
θ	128.91° ± 0.02°
V_{tan}	332 ± 15 km s^{-1}
$(J-H)$[a]	0.121 ± 0.017 mag
$(J-K)$[a]	0.17 ± 0.07 mag
K[a]	14.80 ± 0.07 mag

[a] Magnitudes on the CIT photometric system.

observational properties—distance, luminosity, and effective temperature (T_{eff})—which can be facilitated by parallax measurements. However, while astrometric studies of late-type field dwarfs have provided robust absolute magnitude, T_{eff}, and luminosity scales down to the lowest luminosity brown dwarfs known (Dahn et al. 2002; Tinney et al. 2003; Vrba et al. 2004), parallax measurements for late-type subdwarfs are rare (Monet et al. 1992), and there are no such measurements for any L subdwarfs.

To address this deficiency, we report the first parallax measurement of an L subdwarf, 2MASS J05325346+8246465 (hereafter 2MASS J0532+8246; Burgasser et al. 2003), one of the first and latest type L subdwarfs to be identified. This source is tentatively classified sdL7 due to the similarity of its optical spectrum to those of solar metallicity L7 dwarfs (Burgasser et al. 2007a). Its late spectral type, low estimated temperature ($T_{eff} \approx 1400$–2000 K), and halo kinematics all make 2MASS J0532+8246 a strong candidate halo brown dwarf.

In § 2 we describe astrometric and photometric measurements of 2MASS J0532+8246, conducted as part of the United States Naval Observatory (USNO) infrared astrometry program (Vrba et al. 2004), and compare its absolute photometry to field late-type M, L, and T dwarfs. In § 3 we calculate the bolometric luminosity and T_{eff} of 2MASS J0532+8246 based on our astrometric measurements and broadband spectral and photometric measurements reported in the literature. In § 4 we analyze these results, determining estimates of the physical properties of 2MASS J0532+8246 using evolutionary models from Baraffe et al. (1997, 1998) and Burrows et al. (2001), and examine the kinematics of this source and its Galactic orbit. Results are summarized in § 5.

2. OBSERVATIONS

2.1. *Astrometric Measurements*

Astrometric observations of 2MASS J0532+8246 were obtained with the ASTROCAM near-infrared imager (Fischer et al. 2003) at the USNO Flagstaff Station 61 inch Kaj Straand Astrometric Reflector on 37 nights spanning a ~3 yr period beginning in 2003 February and ending in 2006 February.[7] Each of the observations was made in the H band (1.7 μm), with three dithered exposures of 450–900 s each, depending on seeing conditions (always less than 2.5″), or 1350–2700 s total integration per visit. Data acquisition and astrometric reduction procedures are discussed in detail in Vrba et al. (2004). Note that observations for 2MASS J0532+8246 span a longer baseline than the L and T dwarfs reported in Vrba et al. (2004), so that stable parallaxes in both right ascension and declination could be determined and combined. Twelve stars were employed in the reference frame, and photometric parallaxes for these sources were determined using 2MASS photometry transformed to the CIT system. The correction from relative to absolute parallax was found to be 1.14 ± 0.13 mas.

Final values for the parallax (relative and absolute) and proper-motion solutions for 2MASS J0532+8246 are listed in Table 1. The astrometric distance of this source is 26.7 ± 1.2 pc, within the 10–30 pc range estimated by Burgasser et al. (2003). The proper-motion measurement, 2.6241″ ± 0.0018″ yr^{-1}, is also consistent with, but substantially more accurate than, the previous determination (2.60″ ± 0.15″ yr^{-1}). The USNO measurements confirm the high tangential space velocity of 2MASS J0532+8246, $V_{tan} = 332 \pm 15$ km s^{-1}, over 3 times larger than any of the known "disk" field L dwarfs (Vrba et al. 2004; Schmidt et al. 2007). Combined with its radial velocity ($V_{rad} = -172 \pm 1$ km s^{-1}; Reiners & Basri 2006), we determine local standard of rest (LSR) velocities of $(U, V, W)_{LSR} = (-70, -354, 78) \pm (9, 13, 7)$ km s^{-1}, assuming a LSR solar velocity of (10.00, 5.25, 7.17) km s^{-1} (Dehnen & Binney 1998). The substantial negative V_{LSR} velocity implies that 2MASS J0532+8246 is orbiting in a retrograde motion about the Galactic center, i.e., in the opposite sense of the Galactic disk (assuming that $V_{disk} = 220$ km s^{-1} in galactocentric coordinates; Kerr & Lynden-Bell 1986). This would appear to rule out membership in the thick-disk population (Chiba & Beers 2000), so 2MASS J0532+8246 is likely to be a halo low-mass object. The Galactic orbit of this source is discussed further in § 4.2.

2.2. *Photometric Measurements*

Near-infrared photometric measurements of 2MASS J0532+8246 were also obtained during the course of the astrometric observations in an attempt to improve on existing 2MASS photometry (uncertainties of 0.06, 0.09, and 0.15 mag in J, H, and K_s bands, respectively). The J-, H-, and K-band observations on the CIT system (Guetter et al. 2003) were obtained with ASTROCAM on 2003 October 12 (UT). Conditions were clear with ~0.9″ seeing. Three dithered exposures were obtained in each filter with total integration times of 720, 720, and 1500 s, respectively. The ASTROCAM field of view contained nine stars significantly brighter than 2MASS J0532+8246, with mean 2MASS J, H, and K_s uncertainties of 0.03, 0.04, and 0.07 mag, respectively. 2MASS photometry for these sources were converted to the CIT system using the transformations of Carpenter (2001), which were then employed as "local photometric standards" on the ASTROCAM frames. Aperture photometry of these stars and 2MASS J0532+8246 was then carried out using DAOPHOT in the IRAF[8] environment on each of the individual dithers, and the combined instrumental magnitudes and colors were used to determine transformations to the CIT standard system. Final results for 2MASS J0532+8246 are listed in Table 1. We note that along with reduced errors, the USNO photometry of this source is brighter and somewhat bluer than the 2MASS photometry, albeit within the 3 σ uncertainties of the latter.

2.3. *Examination of Absolute Magnitudes*

2MASS J0532+8246 is the first L subdwarf to have a measured distance; hence, examination of its absolute magnitudes (Table 3) is of some importance in understanding the atmospheric properties

[7] Astrometric observations of 2MASS J0532+8246 were terminated only after a 2006 June cryogenic explosion seriously damaged ASTROCAM. When this instrument is restored to operational status (expected mid-2008), observations will resume for this source and other L and T dwarfs in the USNO infrared astrometric program.

[8] IRAF is distributed by the National Optical Astronomy Observatory, which is operated by the Association of Universities for Research in Astronomy, Inc., under cooperative agreement with the National Science Foundation.

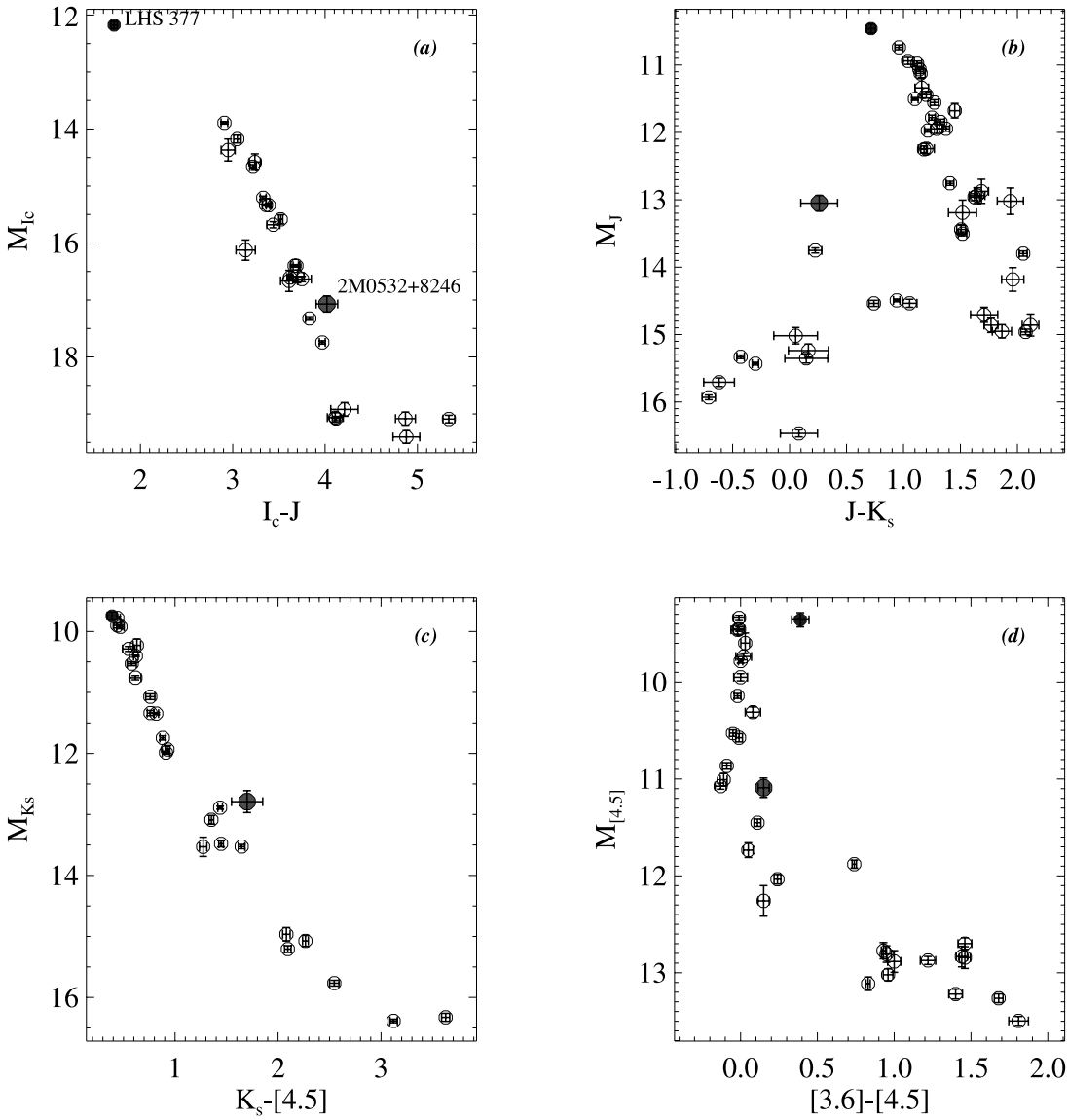

FIG. 1.—Absolute magnitudes vs. color for a sample of field late-type M, L, and T dwarfs, based on red optical and infrared photometry from Monet et al. (1992), Dahn et al. (2002), Burgasser et al. (2003), Patten et al. (2006), and 2MASS; and parallax measurements from Monet et al. (1992), Perryman et al. (1997), Dahn et al. (2002), Tinney et al. (2003), and Vrba et al. (2004). Sources shown are constrained to have color and absolute magnitude uncertainties $\leq$0.2 mag, and to be unresolved. Diagrams shown are: (*a*) M_{I_C} vs. $(I_C - J)$, (*b*) M_J vs. $(J - K_s)$, (*c*) M_{K_s} vs. $(K_s - [4.5])$, and (*d*) $M_{[4.5]}$ vs. $([3.6] - [4.5])$. The location of 2MASS J0532+8246 and the sdM7 LHS 377 are indicated in each panel by filled gray and black circles, respectively. [*See the electronic edition of the Journal for a color version of this figure.*]

of low-temperature metal-poor dwarfs. Figures 1 and 2 display a sample of optical and infrared color/magnitude and spectral type/magnitude diagrams for late-type M, L, and T dwarfs with parallax measurements, including 2MASS J0532+8246. Photometric data were culled from Dahn et al. (2002) and Burgasser et al. (2003) for I_C band (0.8 μm), 2MASS for near-infrared JHK_s, and Patten et al. (2006) for mid-infrared measurements made with the *Spitzer* IRAC instrument (Fazio et al. 2004). Astrometric data are from Perryman et al. (1997), Dahn et al. (2002), Tinney et al. (2003), and Vrba et al. (2004). For the spectral type/magnitude plots, we used published optical spectral types for late-type M and L dwarfs (e.g., Kirkpatrick et al. 1999) and near-infrared spectral types for T dwarfs (e.g., Burgasser et al. 2006). Sources were constrained to have color and magnitude uncertainties no greater than 0.2 mag, and not known to be multiple (Burgasser et al. 2007b and references therein). We also include absolute magnitudes and colors for the sdM7 LHS 377 (Monet et al. 1992; Gizis 1997), until now the latest type subdwarf with a reported parallax measurement.

In general, 2MASS J0532+8246 is somewhat overluminous for both its color and spectral type. This is particularly the case at *J* band, where it is 1–2 mag brighter than the disk L dwarf/T dwarf sequence based on both spectral type and color. Indeed, 2MASS J0532+8246 lies in a relatively unpopulated region in the M_J versus $(J - K_s)$ color/magnitude diagram. The *J*-band opacity in L dwarf photospheres is dominated by absorption from condensates, which gives rise to their red $J - K_s$ colors (Tsuji et al. 1996, 1999; Burrows & Sharp 1999; Ackerman & Marley 2001; Allard et al. 2001). Burgasser et al. (2003, 2007a) and Reiners & Basri (2006) have all speculated that condensate formation may be inhibited in L subdwarf photospheres based on the unexpected strength of gaseous TiO, Ca I, and Ti I features. Reduced condensate opacity allows *J*-band light to escape from deeper and hotter layers, resulting in an overall brightening at these wavelengths

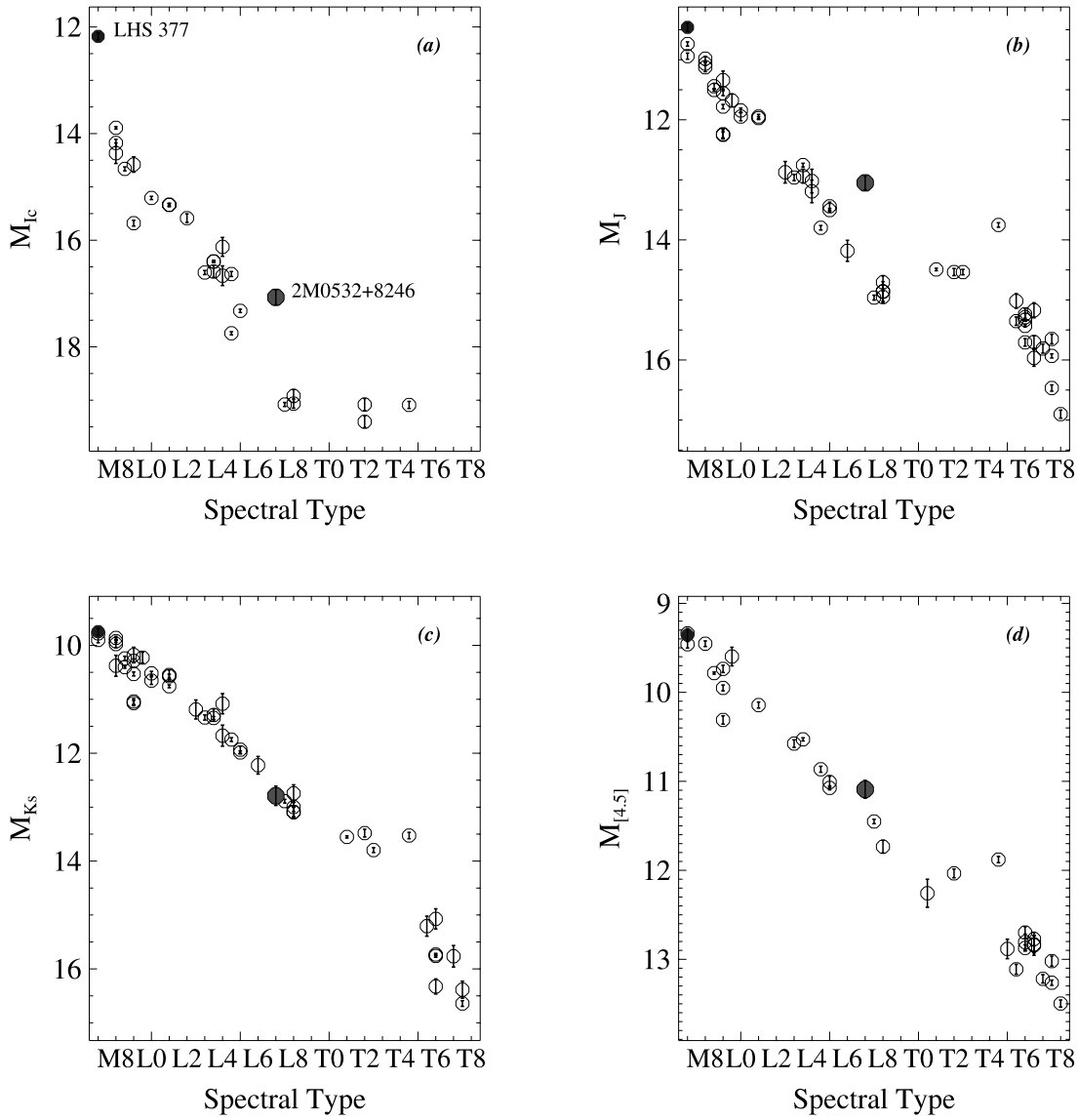

FIG. 2.—Absolute magnitudes vs. spectral type for the same sample described in Fig. 1. Shown are (*a*) M_{I_C}, (*b*) M_J, (*c*) M_{K_s}, and (*d*) $M_{[4.5]}$ vs. optical spectral types for M and L dwarfs (Kirkpatrick et al. 1999), and near-infrared spectral types for T dwarfs (Burgasser et al. 2006). Spectral types of sdM7 and sdL7 are assumed for LHS 377 and 2MASS J0532+8246 (*filled black and dark gray circles, respectively*). [*See the electronic edition of the Journal for a color version of this figure.*]

(Ackerman & Marley 2001). In contrast, *K*-band opacity is dominated by collision-induced H_2 opacity in late-type dwarfs, a species whose absolute abundance is not modified by metallicity. The higher pressure photospheres of old, high surface gravity subdwarfs will in fact increase H_2 opacity. This trend explains why the M_{K_s} magnitude of 2MASS J0532+8246 is consistent with, and perhaps slightly fainter than, those of solar metallicity L7 field dwarfs. Given that the primary deviation in the near-infrared brightness of 2MASS J0532+8246 occurs in the spectral region in which condensate opacity should be dominant, these results provide further support for the idea that condensate formation is inhibited in low-temperature metal-poor atmospheres.

The location of 2MASS J0532+8246 redward and/or above the L dwarf sequence in the M_{I_C} versus $(I_C - J)$ and M_{K_s} versus $(K_s - [4.5])$ color/magnitude diagrams can also be explained by metallicity effects. Reduced *J*-band condensate opacity coupled with residual (albeit reduced) TiO and pressure-broadened K I absorption at I_C band result in slightly redder $(I_C - J)$ colors than comparably classified field dwarfs. This is in contrast to the sdM7 LHS 377, which is brighter at I_C band rather than *J* band as compared to M7 field dwarfs, and hence bluer in $(I_C - J)$. The difference in color peculiarity between these two sources can be attributed to the fact that late M dwarfs are too warm to have significant condensates in their photospheres (Ackerman & Marley 2001), while variations in metal oxide absorption have a greater effect. The $(K_s - [4.5])$ color of 2MASS J0532+8246 is slightly redder than field dwarfs with similar M_{K_s} magnitudes because of enhanced 4.5 μm flux. This region is dominated by metallicity-sensitive molecular CO and H_2O opacity, in contrast to the strong H_2 absorption at K_s. Both 2MASS J0532+8246 and LHS 377 have redder ([3.6] − [4.5]) colors than the dwarf sequence; similar metallicity-induced color effects have also been noted among field T dwarfs (Liebert & Burgasser 2007; Leggett et al. 2007).[9] The red ([3.6] − [4.5]) color of 2MASS J0532+8246

[9] Late-type esdMs also have redder $B - V$ colors at a given M_V magnitude due to similar metal opacity effects (Gizis 1997).

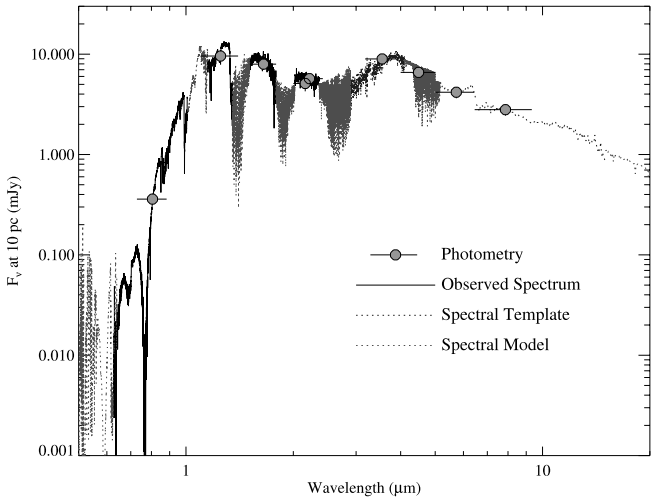

FIG. 3.—Absolute spectral energy distribution (F_ν at 10 pc) of 2MASS J0532+8246 used to calculate its bolometric luminosity. Absolute photometry from Burgasser et al. (2003), 2MASS, Patten et al. (2006), and this paper are indicated by gray circles. Flux-calibrated spectral data from Burgasser et al. (2003) are indicated by black lines. Scaled spectral template data for the L5 2MASS J1507−1627 (Cushing et al. 2006) are indicated by light gray dotted lines. Scaled NEXTGEN spectral model data ($T_{\rm eff} = 2000$ K, $\log g = 5.5$ cgs, and [M/H] = −1.0) from Hauschildt et al. (1999) are indicated by dark gray dotted lines. This hybrid spectrum was integrated to determine a bolometric flux of $(18.2 \pm 2.6) \times 10^{-12}$ ergs cm^{-2} s^{-1}, which includes an estimate of systematic uncertainty. [*See the electronic edition of the Journal for a color version of this figure.*]

may be muted, however, if CH_4 absorption at 3.3 μm, present in mid- and late-type L dwarfs (Noll et al. 2000; Cushing et al. 2005), is also weakened by metallicity effects.

3. BOLOMETRIC LUMINOSITY AND EFFECTIVE TEMPERATURE DETERMINATIONS

Our distance measurement for 2MASS J0532+8246 enables calculation of its bolometric luminosity and $T_{\rm eff}$, through the use of existing spectroscopic and photometric data spanning 0.6–15 μm. Our baseline calculation, illustrated in Figure 3, was constructed as follows. First, near-infrared spectral data for 2MASS J0532+8246 from Burgasser et al. (2003) were piecewise scaled to absolute 2MASS *J*, *H*, and USNO *K*-band magnitudes (Table 3). Gaps in the H_2O bands and the 1 μm peak were substituted by a NEXTGEN spectral model (Hauschildt et al. 1999) with parameters $T_{\rm eff} = 2000$ K, $\log g = 5.5$, [M/H] = −1.0 dex, scaled to match the flux-calibrated spectral data in the near-infrared peaks. Red optical spectral data for 2MASS J0532+8246 were scaled to the absolute I_C magnitude of this source (Burgasser et al. 2003). As there are no reported spectral data for 2MASS J0532+8246 at longer wavelengths, we used a spectral template based on data for the L5 dwarf 2MASS J15074769−1627386 (hereafter 2MASS J1507−1627; Reid et al. 2000; Cushing et al. 2006), spanning the 2.9–4.1 and 5.2–15.4 μm regions and piecewise scaled to match the absolute 3.6, 5.8, and 8.0 μm *Spitzer* IRAC photometry of 2MASS J0532+8246 (Patten et al. 2006). Flux calibration of these data was done using the appropriate correction factor for IRAC photometry as discussed in Cushing et al. (2006). The 2.4–2.9 and 4.1–5.2 μm gaps were again replaced with theoretical model spectra, scaled to overlap with the template spectra and to match absolute 4.5 μm photometry of 2MASS J0532+8246. Short- (0.1 μm $< \lambda <$ 0.6 μm) and long- (15 μm $< \lambda <$ 1000 μm) wavelength regions were calculated by scaling the NEXTGEN spectral model to the observed and template spectra, respectively.

The resulting broad spectral energy distribution was then integrated to determine the total spectral flux, with nominal uncertainties based on the absolute photometry, including astrometric uncertainties. To examine systematic effects, we repeated our analysis replacing the NEXTGEN model with a $T_{\rm eff} = 1700$ K, $\log g = 5.5$, [M/H] = −0.5 condensate cloud model from Burrows et al. (2006; hereafter Tucson model), as well as linearly interpolating over gaps in the observed and template spectral data.

Table 2 provides a breakdown of the total fluxes of 2MASS J0532+8246 in five spectral regions, with comparisons between the different computational methods. As expected, the bulk of the spectral flux for this late-type dwarf arises at infrared wavelengths (∼93%), with the 1.0–2.9 μm region encompassing almost 70% of the total light. Differences between the computational methods are generally less than the formal uncertainties, except in the shortest and longest wavelength regions, which fortuitously contribute negligibly to the aggregate flux (<0.25%). Bolometric flux values computed using the two spectral models and linear interpolation are within 3 σ of each other, with our baseline calculation providing the median value. We therefore use this value as the measured bolometric flux, and propagate the estimated systematic error (∼14%) into our final uncertainties.

We determine an absolute bolometric flux of $(18.2 \pm 2.6) \times 10^{-12}$ ergs cm^{-2} s^{-1} for 2MASS J0532+8246, which translates

TABLE 2
INTEGRATED SPECTRAL FLUX FOR 2MASS J0532+8246

Wavelength Range (μm)	Flux (10^{-12} ergs cm^{-2} s^{-1})	Fraction (%)	Method
0.01–0.64	**0.031 ± 0.003**	0.17	NEXTGEN Model, 2MASS photometry
	0.096 ± 0.009	...	Linear extrapolation, 2MASS photometry
0.64–1.0	**1.24 ± 0.11**	6.81	Observed spectrum, 2MASS photometry
1.0–2.9	**12.6 ± 0.5**	69.45	Observed spectrum, NEXTGEN model, 2MASS/USNO photometry
	12.4 ± 0.4	...	Observed spectrum, Tucson model, 2MASS/USNO photometry
	12.7 ± 0.4	...	Observed spectrum, spectral template, linear interpolation, 2MASS/USNO photometry
2.9–15	**4.27 ± 0.19**	23.52	Spectral template, NEXTGEN model, IRAC photometry
	4.4 ± 0.5	...	Spectral template, Tucson model, IRAC photometry
	4.39 ± 0.12	...	Spectral template, linear interpolation, IRAC photometry
15–1000	**0.0096 ± 0.0009**	0.05	NEXTGEN model, IRAC photometry
	0.077 ± 0.007	...	Raleigh-Jeans tail, IRAC photometry
0.1–1000	**18.2 ± 1.7**	100.00	Observations + NEXTGEN model
	18.0 ± 1.8	...	Observations + Tucson model
	18.5 ± 1.7	...	Observations + linear interpolation

NOTE.—Values listed in bold represent our baseline calculation.

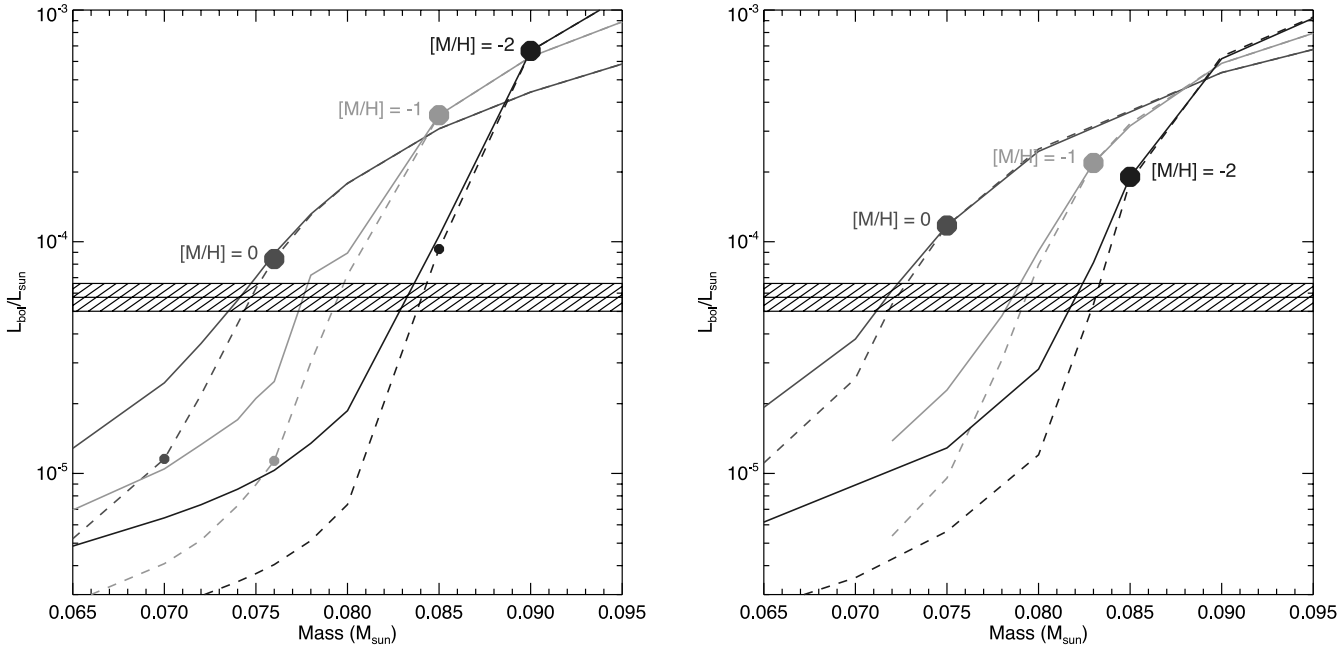

FIG. 4.—Theoretical mass/luminosity relations for low-mass stars and brown dwarfs, based on evolutionary models from Burrows et al. (2001; *left*) and Baraffe et al. (1997, 1998; *right*). Models are shown for ages of 5 (*solid lines*) and 10 Gyr (*dashed lines*), and metallicities [M/H] = 0 (*dark gray lines*), −1 (*light gray lines*), and −2 dex (*black lines*). The limits at which 50% (*small circles in left panel*) and 99% (*large circles in both panels*) of the total luminosity originates from core hydrogen fusion are indicated. The measured luminosity of 2MASS J0532+8246 is indicated by the hatched region (1 σ uncertainties), and falls below the 99% limit for all models, but above the 50% limit for [M/H] $\gtrsim -1$ models of Burrows et al. (2001). Note that each model predicts a slightly different mass for 2MASS J0532+8246, varying primarily by metallicity but according to evolutionary calculation as well. [*See the electronic edition of the Journal for a color version of this figure.*]

into a bolometric luminosity of $\log L/L_{\rm bol} = -4.24 \pm 0.06$, or $M_{\rm bol} = 15.35 \pm 0.16$. This is comparable to mid-type L dwarfs like 2MASS J1507−1627 ($M_{\rm bol} = 15.41 \pm 0.13$; Vrba et al. 2004), and is roughly half a magnitude more luminous than the average L7 dwarf. 2MASS J0532+8246 is nevertheless over 10 times less luminous than the next coolest subdwarf with a parallax measurement, sdM7 LHS 377 ($\log L/L_{\rm bol} = -3.11 \pm 0.02$; Leggett et al. 2000). Bolometric corrections ($BC_b \equiv M_{\rm bol} - M_b$) at J and K were determined as $BC_J = 2.30 \pm 0.08$ and $BC_K = 2.68 \pm 0.09$. The latter is ∼0.5 mag smaller than comparable values computed for L6–L8 field dwarfs, further illustrating the substantial redistribution of flux from this metal-poor source.

An effective temperature for 2MASS J0532+8246 can be estimated assuming that this source is likely older than ∼5 Gyr based on its kinematics, and has a mass near the hydrogen-burning limit (0.05–0.09 $M_\odot$, depending on metallicity; see § 4.1). These assumptions imply a radius of 0.096 ± 0.015 $R_\odot$ based on the solar metallicity evolutionary models of Burrows et al. (2001) and Baraffe et al. (2002) and yields $T_{\rm eff} = 1600 \pm 300$ K, where the uncertainty is entirely dominated by the uncertainty in the radius. If we include the measured luminosity (including 3 σ uncertainty) as an additional constraint on these models, a more refined radius estimate of 0.084 ± 0.003 $R_\odot$ is obtained, corresponding to $T_{\rm eff} = 1730 \pm 90$ K. Again, this is comparable to temperatures for mid-type L dwarfs (Vrba et al. 2004; Golimowski et al. 2004) and is nearly 1200 K cooler than LHS 377 (Leggett et al. 2000).

4. DISCUSSION

4.1. *The Substellar Nature of 2MASS J0532+8246*

While parallax and bolometric luminosity measurements are able to constrain some of the atmospheric properties of 2MASS J0532+8246, they do not directly address the question of whether this source is substellar. For this we require comparison to evolutionary models: in particular, models incorporating subsolar metallicities. The reduced opacity of a metal-poor atmosphere results in more rapid cooling; hence, the luminosity of a metal-poor brown dwarf will be lower than that of a solar metallicity brown dwarf with the same mass and age, while the hydrogen-burning minimum-mass limit increases for lower metallicities (e.g., D'Antona & Mazzitelli 1985). Figure 4 illustrates these trends by comparing theoretical mass/luminosity relations from Burrows et al. (2001) and Baraffe et al. (1997, 1998) spanning the hydrogen-burning limit for ages of 5 and 10 Gyr and metallicities [M/H] = 0, −1, and −2 dex. The limits at which 50% and 99% of the luminosity is generated from core hydrogen fusion at 10 Gyr are indicated; note how these limits shift to higher masses and luminosities for lower metallicity models. The luminosity of 2MASS J0532+8246 falls below the 99% limits for all models shown, as well as for intermediate and lower metallicities. This appears to confirm 2MASS J0532+8246 as a brown dwarf, incapable of sustaining its luminosity by core hydrogen fusion alone. However, note that for [M/H] $\gtrsim -1$, hydrogen fusion provides over half of the energy emitted, so 2MASS J0532+8246 is fairly close to the stellar/substellar boundary. Indeed, if its metallicity is sufficiently high, this object may eventually cool to the point at which its lower luminosity is sustained by core fusion, changing this low-mass brown dwarf into a star.

The luminosity of 2MASS J0532+8246 falls on a particularly steep section of the mass/luminosity relations shown, enabling relatively tight (1%), albeit model-dependent, constraints on the mass of this source for a given metallicity. However, the variation in the derived mass for the metallicity range shown is considerably larger, ranging from 0.0744 to 0.0835 $M_\odot$ for [M/H] = 0 to −2 for the Burrows et al. (2001) models (these values are consistent with mass estimates based on the Baraffe et al. [1997, 1998] models). Our best guess for the metallicity of this source, [M/H] = −1 (Burgasser et al. 2007a; see also Scholz et al. 2004), implies

TABLE 3
PROPERTIES OF 2MASS J0532+8246

Parameter	Value	References
α[a]	$05^h32^m53.46^s$	1
δ[a]	$+82°46'46.5''$	1
μ	$2.6241'' \pm 0.0018''$ yr^{-1}	2
θ	$128.91° \pm 0.02°$	2
Spectral type	sdL7	3, 4
d	26.7 ± 1.2 pc	2
$M-m$	-2.13 ± 0.10 mag	2
$(U, V, W)_{LSR}$	$(-70, -354, 78) \pm (9, 13, 7)$ km s^{-1}	2, 5
Kinematic population	Halo	2
$\log L_{bol}/L_\odot$	-4.24 ± 0.06	1
M_{bol}	15.35 ± 0.16 mag	2
M_{I_c}	17.07 ± 0.14 mag	2, 3
M_J	13.05 ± 0.12 mag	1, 2
M_H	12.77 ± 0.13 mag	1, 2
M_{K_s}	12.79 ± 0.18 mag	1, 2
M_K	12.67 ± 0.12 mag	2
$M_{[3.6]}$	11.24 ± 0.10 mag	2, 6
$M_{[4.5]}$	11.09 ± 0.10 mag	2, 6
$M_{[5.8]}$	11.10 ± 0.14 mag	2, 6
$M_{[8.0]}$	10.90 ± 0.14 mag	2, 6
BC$_J$	2.30 ± 0.08 mag	1, 2
BC$_K$	2.68 ± 0.09 mag	2
T_{eff}	1730 ± 90 K	2, 7, 8
Mass[b]	$0.0744 \pm 0.0009\ M_\odot$	2, 7
	$0.0783 \pm 0.0013\ M_\odot$	2, 7
	$0.0835 \pm 0.0008\ M_\odot$	2, 7

[a] J2000.0 coordinates at epoch 1999 March 1 (UT).
[b] Mass estimates for [M/H] = 0, −1, and −2 based on the evolutionary models of Burrows et al. (2001) assuming an age of 5–10 Gyr. Values are consistent with those derived using the Baraffe et al. (1997, 1998) models, within the estimated uncertainties.

REFERENCES.—(1) 2MASS; (2) this paper; (3) Burgasser et al. 2003; (4) Burgasser et al. 2007a; (5) Reiners & Basri 2006; (6) Patten et al. 2006; (7) Burrows et al. 2001; (8) Baraffe et al. 2002.

a mass of $0.0783 \pm 0.0013\ M_\odot$ ($0.0788 \pm 0.0006\ M_\odot$ for the Baraffe et al. [1997, 1998] models). However, it is clear that the unknown metallicity of 2MASS J0532+8246 remains the largest source of uncertainty in characterizing its physical properties.

4.2. *The Galactic Orbit of 2MASS J0532+8246*

The kinematics of 2MASS J0532+8246 argue strongly for membership in the Galactic halo, but was this source formed early in the Galaxy, or was it tidally stripped from one of the Galaxy's dwarf satellites during a merging event? To examine this question, we calculated a probable orbit for 2MASS J0532+8246 based on its measured kinematics, distance, and 2MASS coordinates (epoch 1999 March 1 UT; Table 3). We used the Galactic mass model of Dauphole & Colin (1995) and a Runge-Kutta fourth-order integrator; see Lépine et al. (2002) for details. Figure 5 displays the results of this calculation, projecting the ~110 Myr galactocentric orbit in cylindrical coordinates, as well as the evolution of Galactic radius and vertical scale height over time. 2MASS J0532+8246 appears to have a relatively eccentric orbit, moving between roughly 3 and 8.5 kpc of the Galactic center ($e \approx 0.5$). The vertical scale height of its orbit extends ~2 kpc above and below the Galactic plane.

The orbital characteristics of 2MASS J0532+8246 appear to be inconsistent with tidal capture from an external system, as this source generally remains interior to the solar Galactic orbit. Rather, it is likely to be a member of the Galaxy's inner flattened

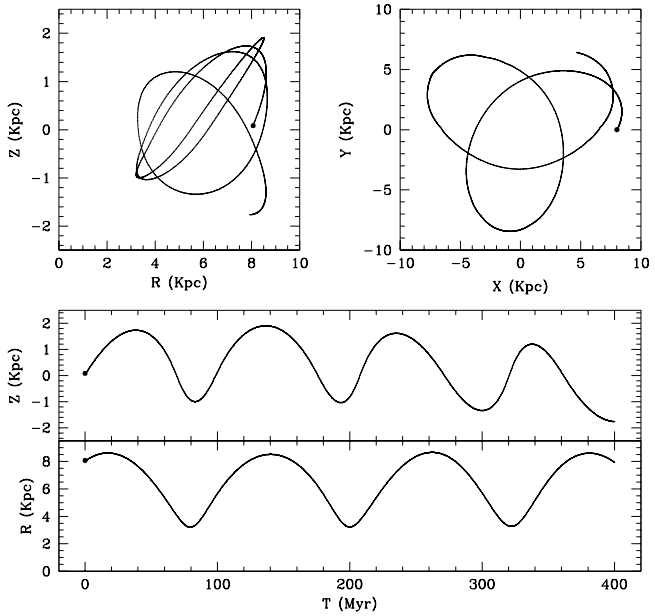

FIG. 5.—Integrated Galactic orbit of 2MASS J0532+8246, based on its $(U, V, W)_{LSR}$ space velocities, 2MASS coordinates, and measured distance. The orbit was calculated using the Galactic mass model of Dauphole & Colin (1995) and a Runge-Kutta fourth-order integrator. The top left panel shows the projected orbit perpendicular to the Galactic disk, with the Galactic plane at $Z = 0$. The top right panel shows the projected orbit in the plane of the Galaxy; the sense of the Galactic disk rotation is clockwise. The bottom panels show the temporal evolution of the orbit in galactocentric cylindrical coordinates over a period of 400 Myr starting from the current epoch (roughly four revolutions).

halo (Sommer-Larsen & Zhen 1990), indicating formation from the early building blocks of the Galaxy (e.g., Norris 1994; Carney et al. 1996). The substantial retrograde motion of 2MASS J0532+8246 also argues against formation and (violent) ejection from the inner disk. In other words, 2MASS J0532+8246 is likely to be quite old. However, this does not provide a robust constraint on its metallicity. Mean eccentricity/metallicity relations by Carney et al. (1996) and Chiba & Beers (2000) suggest $[Fe/H] \lesssim -1$, but the latter study also finds no clear correlation between orbital eccentricity and metallicity for $[Fe/H] < -0.8$. The chemical abundances present in the atmosphere of 2MASS J0532+8246, a necessary constraint for mass estimation, must be determined through other means, most likely spectral modeling.

5. SUMMARY

We have presented the first parallax and luminosity measurements for an L subdwarf, the sdL7 2MASS J0532+8246. The derived parameters, summarized in Table 3, confirm the low-luminosity, low-temperature nature of this source, similar in both respects to mid-type field L dwarfs. Examination of absolute photometry indicates that this source is substantially brighter at J band than comparable solar metallicity field dwarfs, consistent with reduced condensate opacity as previously suggested by optical spectroscopy. The low luminosity of 2MASS J0532+8246, $\log L_{bol}/L_\odot = -4.24 \pm 0.06$, compared to theoretical evolutionary models also confirms the substellar nature of this source ($M \approx 0.078\ M_\odot$, assuming $[M/H] = -1$), although it is probably still fusing hydrogen at a low level in its core. Its kinematics are consistent with membership in the inner halo population, making this source the first *bona fide* halo brown dwarf.

Further investigation of 2MASS J0532+8246 should be directed toward determining its metallicity and chemical abundances. As

discussed in § 4.1, uncertainty in the estimated mass of this source is dominated by its unknown metallicity. High-resolution spectroscopy (e.g., Reiners & Basri 2006) and accurate spectral modeling can improve mass constraints, although such analysis must also provide a consistent luminosity determination (cf. Smith et al. 2003). Independent determination of both metallicity and mass could also provide an important empirical test on the evolutionary models themselves, and thus one of the few constraints on interior brown dwarf physics (in addition to radii measurements; e.g., Stassun et al. 2006). Studies of metallicity effects in the physical and observational properties of low-mass stars and brown dwarfs will also benefit from the measurement of parallaxes for additional late-type subdwarfs, to fill the gap between LHS 377 (sdM7) and 2MASS J0532+8246 (sdL7). Such observations should be of high priority, as detailed studies of metallicity effects in the atmospheric properties and evolution of the lowest luminosity stars and brown dwarfs are currently limited by the absence of these data.

The authors would like to thank I. Baraffe and A. Burrows for making available electronic versions of their evolutionary models for our analysis, and M. Cushing for making available his spectral data for 2MASS J1507−1627. We also thank J. Bochanski for additional comments to the manuscript and J. Gizis for his prompt review. This publication makes use of data from the Two Micron All Sky Survey (2MASS), which is a joint project of the University of Massachusetts and the Infrared Processing and Analysis Center, and funded by the National Aeronautics and Space Administration and the National Science Foundation. 2MASS data were obtained from the NASA/IPAC Infrared Science Archive, which is operated by the Jet Propulsion Laboratory, California Institute of Technology, under contract with the National Aeronautics and Space Administration. This research has benefitted from the M, L, and T dwarf compendium housed at http://dwarfarchives.org and maintained by Chris Gelino, Davy Kirkpatrick, and Adam Burgasser; and the VLM Binary Archive maintained by N. Siegler at http://www.vlmbinaries.org.

REFERENCES

Ackerman, A. S., & Marley, M. S. 2001, ApJ, 556, 872
Allard, F., Hauschildt, P. H., Alexander, D. R., Tamanai, A., & Schweitzer, A. 2001, ApJ, 556, 357
Baraffe, I., Chabrier, G., Allard, F., & Hauschildt, P. H. 1997, A&A, 327, 1054
———. 1998, A&A, 337, 403
Baraffe, I., Chabrier, G., Barman, T. S., Allard, F., & Hauschildt, P. H. 2003, A&A, 402, 701
Bildsten, L., Brown, E. F., Matzner, C. D., & Ushomirsky, G. 1997, ApJ, 482, 442
Borysow, A., Jørgensen, U. G., & Zheng, C. 1997, A&A, 324, 185
Boss, A. P. 2006, ApJ, 644, L79
Burgasser, A. J. 2004, ApJ, 614, L73
Burgasser, A. J., Cruz, K. L., & Kirkpatrick, J. D. 2007a, ApJ, 657, 494
Burgasser, A. J., Geballe, T. R., Leggett, S. K., Kirkpatrick, J. D., & Golimowski, D. A. 2006, ApJ, 637, 1067
Burgasser, A. J., Kirkpatrick, J. D., & Lépine, S. 2005, in Proc. 13th Cambridge Workshop on Cool Stars, Stellar Systems, and the Sun, ed. F. Favata, G. A. J. Hussain, & B. Battrick (ESA-SP 560; Noordwijk: ESA), 237
Burgasser, A. J., Reid, I. N., Siegler, N., Close, L. M., Allen, P., Lowrance, P. J., & Gizis, J. E. 2007b, in Planets and Protostars V, ed. B. Reipurth, D. Jewitt, & K. Keil (Tucson: Univ. Arizona Press), 427
Burgasser, A. J., et al. 2003, ApJ, 592, 1186
Burrows, A., Hubbard, W. B., Lunine, J. I., & Liebert, J. 2001, Rev. Mod. Phys., 73, 719
Burrows, A., & Sharp, C. M. 1999, ApJ, 512, 843
Burrows, A., Sudarsky, D., & Hubeny, I. 2006, ApJ, 640, 1063
Carney, B. W., Laird, J. B., Latham, D. W., & Aguilar, L. A. 1996, AJ, 112, 668
Carpenter, J. M. 2001, AJ, 121, 2851
Chiba, M., & Beers, T. C. 2000, AJ, 119, 2843
Cruz, K. L., Reid, I. N., Liebert, J., Kirkpatrick, J. D., & Lowrance, P. J. 2003, AJ, 126, 2421
Cruz, K. L., et al. 2007, AJ, 133, 439
Cushing, M. C., Rayner, J. T., & Vacca, W. D. 2005, ApJ, 623, 1115
Cushing, M. C., et al. 2006, ApJ, 648, 614
Dahn, C. C., Liebert, J., Harris, H. C., & Guetter, H. H. 1995, in The Bottom of the Main Sequence—and Beyond, ed. C. G. Tinney (Berlin: Springer), 239
Dahn, C. C., et al. 2002, AJ, 124, 1170
D'Antona, F., & Mazzitelli, I. 1985, ApJ, 296, 502
Dauphole, B., & Colin, J. 1995, A&A, 300, 117
Dehnen, W., & Binney, J. J. 1998, MNRAS, 298, 387
Digby, A. P., Hambly, N. C., Cooke, J. A., Reid, I. N., & Cannon, R. D. 2003, MNRAS, 344, 583
Epchtein, N., et al. 1997, Messenger, 87, 27
Fazio, G. G., et al. 2004, ApJS, 154, 10
Fischer, J., et al. 2003, Proc. SPIE, 4841, 564
Gizis, J. E. 1997, AJ, 113, 806
Golimowski, D. A., et al. 2004, AJ, 127, 3516
Guetter, H. H., Vrba, F. J., Henden, A. A., & Luginbuhl, C. B. 2003, AJ, 125, 3344
Hauschildt, P. H., Allard, F., & Baron, E. 1999, ApJ, 512, 377
Helling, C., Klein, R., Woitke, R., Nowak, U., & Sedlmayr, E. 2004, A&A, 423, 657
Kerr, F. J., & Lynden-Bell, D. 1986, MNRAS, 221, 1023
Kirkpatrick, J. D. 2005, ARA&A, 43, 195
Kirkpatrick, J. D., Barman, T. S., Burgasser, A. J., McGovern, M. R., McLean, I. S., Tinney, C. G., & Lowrance, P. J. 2006, ApJ, 639, 1120
Kirkpatrick, J. D., et al. 1999, ApJ, 519, 802
Knapp, G., et al. 2004, AJ, 127, 3553
Laughlin, G., Bodenheimer, P., & Adams, F. C. 1997, ApJ, 482, 420
Leggett, S. K., Allard, F., Dahn, C., Hauschildt, P. H., Kerr, T. H., & Rayner, J. 2000, ApJ, 535, 965
Leggett, S. K., Saumon, D., Marley, M. S., Geballe, T. R., Golimowski, D. A., Stephens, D., & Fan, X. 2007, ApJ, 655, 1079
Lépine, S., Rich, R. M., Neill, J. D., Caulet, A., & Shara, M. M. 2002, ApJ, 581, L47
Lépine, S., Rich, R. M., & Shara, M. M. 2003, ApJ, 591, L49
Liebert, J., & Burgasser, A. J. 2007, ApJ, 655, 522
Linsky, J. L. 1969, ApJ, 156, 989
Lodders, K. 2002, ApJ, 577, 974
Luhman, K. L., Joergens, V., Lada, C., Muzerolle, J., Pascucci, I., & White, R. 2007, in Planets and Protostars V, ed. B. Reipurth, D. Jewitt, & K. Keil (Tucson: Univ. Arizona Press), 443
Monet, D. G., Dahn, C. C., Vrba, F. J., Harris, H. C., Pier, J. R., Luginbuhl, C. B., & Ables, H. D. 1992, AJ, 103, 638
Mould, J. R. 1976, ApJ, 207, 535
Noll, K. S., Geballe, T. R., Leggett, S. K., & Marley, M. S. 2000, ApJ, 541, L75
Norris, J. E. 1994, ApJ, 431, 645
Patten, B. M., et al. 2006, ApJ, 651, 502
Perryman, M. A. C., et al. 1997, A&A, 323, L49
Reid, I. N., Kirkpatrick, J. D., Gizis, J. E., Dahn, C. C., Monet, D. G., Williams, R. J., Liebert, J., & Burgasser, A. J. 2000, AJ, 119, 369
Reid, I. N., Kirkpatrick, J. D., Liebert, J., Gizis, J. E., Dahn, C. C., & Monet, D. G. 2002, AJ, 124, 519
Reiners, A., & Basri, G. 2006, AJ, 131, 1806
Saumon, D., Bergeron, P., Lunine, J. I., Hubbard, W. B., & Burrows, A. 1994, ApJ, 424, 333
Schmidt, S. J., Cruz, K. L., Bongiorno, B. J., Liebert, J., & Reid, I. N. 2007, AJ, 133, 2258
Scholz, R.-D., Lodieu, N., Ibata, R., Bienaymé, O., Irwin, M., McCaughrean, M. J., & Schwope, A. 2004, MNRAS, 347, 685
Skrutskie, M. F., et al. 2006, AJ, 131, 1163
Smith, V. V., et al. 2003, ApJ, 599, L107
Sommer-Larsen, J., & Zhen, C. 1990, MNRAS, 242, 10
Stassun, K., Mathieu, R. D., Vaz, L. P. R., Valenti, J. A., & Gomez, Y. 2006, Nature, 440, 311
Stauffer, J. R., Schultz, G., & Kirkpatrick, J. D. 1998, ApJ, 499, L199
Tarter, J. C., et al. 2007, Astrobiology, 7, 30
Tinney, C. G., Burgasser, A. J., & Kirkpatrick, J. D. 2003, AJ, 126, 975
Tsuji, T., Ohnaka, K., & Aoki, W. 1996, A&A, 305, L1
———. 1999, ApJ, 520, L119
Vrba, F. J., et al. 2004, AJ, 127, 2948
York, D. G., et al. 2000, AJ, 120, 1579